Journal of Water Process Engineering 40 (2021) 101931

Contents lists available at ScienceDirect

Journal of Water Process Engineering

journal homepage: www.elsevier.com/locate/jwpe

The comprehensive evaluation model and optimization selection of activated carbon in the O_3-BAC treatment process

Zhou Yu[a], Li Weiying[a,*], Qi Wanqi[a], Chen Sheng[a], Tan Qiaowen[a], Wei Zhongqing[b], Gong Longcong[c], Chen Junyu[d], Zhou Wenying[e]

[a] *School of Environmental Science and Engineering, Tongji University, Shanghai, 200092, China*
[b] *Fuzhou Water Affairs Investment Development Co., Ltd., Fuzhou, 350000, China*
[c] *Fuzhou Water Co., Ltd., Fuzhou, 350000, China*
[d] *Xiamen Urban Planning and Design Institute, Xiamen, 361001, China*
[e] *Taiyuan Water Authority, Taiyuan, 030000, China*

ARTICLE INFO

Keywords:
Activated
Carbon
Optimization
Advanced water treatment process
Static adsorption
Dynamic adsorption

ABSTRACT

Severe organic pollution in surface water worldwide has put forward higher requirements for new water treatment technologies. Due to the characteristics of large specific surface areas and strong adsorption of organic matters, granular activated carbon has been widely used in water treatment. Currently, little research has been carried out on comprehensive evaluation models for the adsorption and hardness of activated carbon, coursing in a lack of a scientific and comprehensive selection process. Twenty-one kinds of activated carbon (briquetted carbon, cylindrical carbon, cylindrical broken carbon, and broken carbon) produced by seven companies were selected in this study. A comprehensive evaluation model of activated carbon water purification performance was developed. This study not only contained static and dynamic adsorption tests but also included hardness characteristic analysis, and the analytic hierarchy process (AHP) was used to determine the weight of each factor. The results indicated that briquetted carbon performed best in terms of comprehensive performance of activated carbon, to be followed by cylindrical carbon, cylindrical broken carbon, and broken carbon consecutively. Owing to the highest total pore volume (0.581 $m^3\ g^{-1}$) and the highest content of oxygen-containing functional groups, the best performance of briquetted carbon was corroborated by the analysis of physicochemical properties, and the model was reasonable. The research provides a theoretical basis that has important implications for the optimization selection of activated carbon.

1. Introduction

More and more surface water sources have been polluted by industrial, livestock, and agricultural wastewater discharge. Increases in organic, inorganic, and microbial contamination in source water bring in concern of water quality [1], including color, taste, odor, biological instability as well as disinfection byproducts (DBPs) [2–7]. Thus, drinking water safety has become a priority for environmental communities worldwide. The water treatment process plays an essential role in reducing serious illnesses associated with waterborne diseases. Although traditional water treatment processes are excellent for the removal of some contaminants such as suspended solids, colloidal substances, and bacteria from water, they are still unable to satisfy the requirements of progressively higher drinking water quality standards, especially with regard to the removal of organic and emerging contaminants [8–10]. Due to the high specific surface area and hydrophobic interactions as compared to conventional materials, activated carbon shows high potential for controlling heavy metals, organic pollutants, and microorganism removal in drinking water [11–13] and effectively improve water quality [14], the ozone-activated carbon has been widely used in water purification processes [15]. The granular activated carbon (GAC) has been listed as the most effective technique to deal with 51 organic pollutants in the United States Environmental Protection Agency (USEPA) Drinking Water Standard [16].

The selection of granular activated carbon and its operation and maintenance has become the research hotspots in the ozone activated carbon process [17], the basis of its selection and parameter optimization is crucial. At present, most researchers consider the evaluation of a

* Corresponding author.
E-mail address: 123lwyktz@tongji.edu.cn (W. Li).

https://doi.org/10.1016/j.jwpe.2021.101931
Received 14 December 2020; Received in revised form 12 January 2021; Accepted 13 January 2021
Available online 5 February 2021

Table 1
Number of activated carbon samples.

Category / Companies	1 (Briquetted carbon)	2 (Cylindrical carbon)	3 (Cylindrical broken carbon)	4 (Broken carbon)
A		A2	A3	
B	B1-1, B1-2		B3-1, B3-2	
C	C1	C2	C3	C4
D			D3	
E	E1	E2	E3	E4
F		F2	F3	
G	G1	G2	G3	G4

Note: The letter represents the production enterprise, the number after the letter represents the type of carbon, and the number after the "-" means the type of activated carbon in the same category.

single type of activated carbon, mainly based on the physical properties (specific surface area, pore-volume, particle size and strength, ash content, water content, loading density, etc.), and the indicators of adsorption capacity (iodine value, methylene blue [18,19], carbon tetrachloride adsorption capacity, etc.) [20,21]. However, there are many different types of activated carbon. The evaluation methods of the characteristics and removal performance of activated carbon have not been comprehensively investigated, leading to the lack of scientific and overall selection of carbon species.

Based on static and dynamic adsorption assays, combined with the hardness characteristics analyses, we conducted a bench experiment to select excellent activated carbon in this paper. It developed a comprehensive evaluation method of the performance of activated carbon for water purification.

2. Experimental methods and materials

2.1. Experimental materials

Twenty-one kinds of activated carbon (including briquetted carbon, cylindrical carbon, cylindrical broken carbon, and broken carbon) produced by seven companies were selected. As shown in Table 1, they were numbered in accordance with the manufacturers and their categories to carry out a test of blind selection. The corresponding manufacturing information was shown in Table S1.

2.2. The static adsorption assay

Static adsorption includes iodine adsorption value and methylene blue adsorption value. The iodine adsorption value was determined following the "Test Method for Granular Activated Carbon From Coal-Determination of iodine adsorption" (GB/T 7702.7-2008) [22], and the determination of the methylene blue adsorption value was determined following "Test Method for Granular Activated Carbon From Coal-Determination of methylene blue adsorption" (GB/T 7702.6-2008) [23,24].

2.3. The dynamic adsorption assay

The device for the activated carbon dynamic adsorption consisted of a regulating water tank, a peristaltic pump (River YZ15), and an activated carbon column, as shown in Fig. 1. The activated carbon column has an inner diameter of 15 mm and a length of 600 mm. From bottom to top, 10−20 mm gravel (particle size 6−8 mm) and 300 mm optional granular activated carbon were sequentially packed. Stone and optional granular activated carbon were washed with distilled water before filling. The wet packing method was specified for filling.

The tap water was used as feedwater, and sodium thiosulfate was added to the tap water (1.2:1) to neutralize the remaining chlorine in this paper. The water flowed past the activated carbon column from top to bottom, as shown in Fig. 1. The flow rate was 9 m/h. Water quality parameters, including turbidity, UV_{254}, and DOC, were tested from the inlet and outlet water.

2.4. The hardness assay

The hardness of activated carbon was carried out, according to the "Test Method for Granular Activated Carbon from Coal-Determination of Hardness" (GB/T 7702.3-2008) [25]. The activated carbon sample was put into a unique instrument equipped with a certain number of stainless-steel balls, rotated and regularly beat. The sample's mass retained on the assay sieve after the assay accounts for the percentage of the sample's total mass as the hardness of the activated carbon.

2.5. Detection of pore size and surface area of activated carbon

Activated carbon pore size and surface area parameters were detected by the constant temperature gas adsorption method. According to BET (Brunauer-Emmett-Teller) and t-plot curves, the specific surface area, micropore specific surface area, and pore volume of activated carbon were obtained. The specific surface area and pore analysis of activated carbon adopt Micromeritics, with the model ASAP 2020 V4.03.

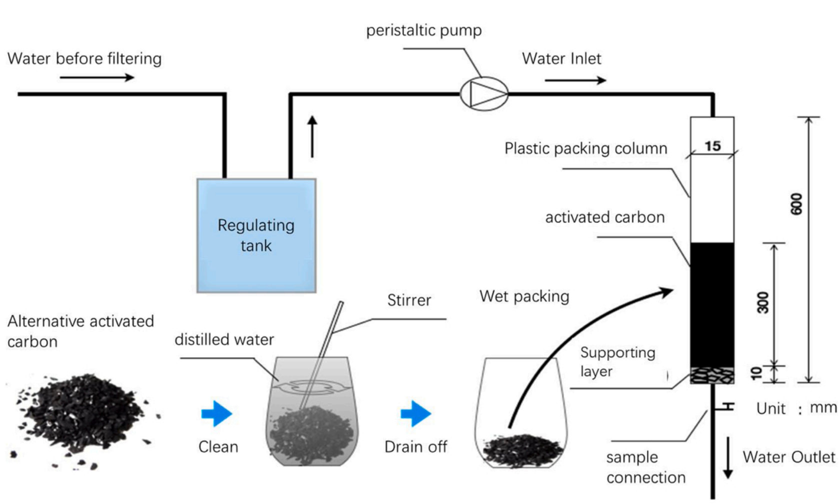

Fig. 1. The device for the activated carbon dynamic adsorption.

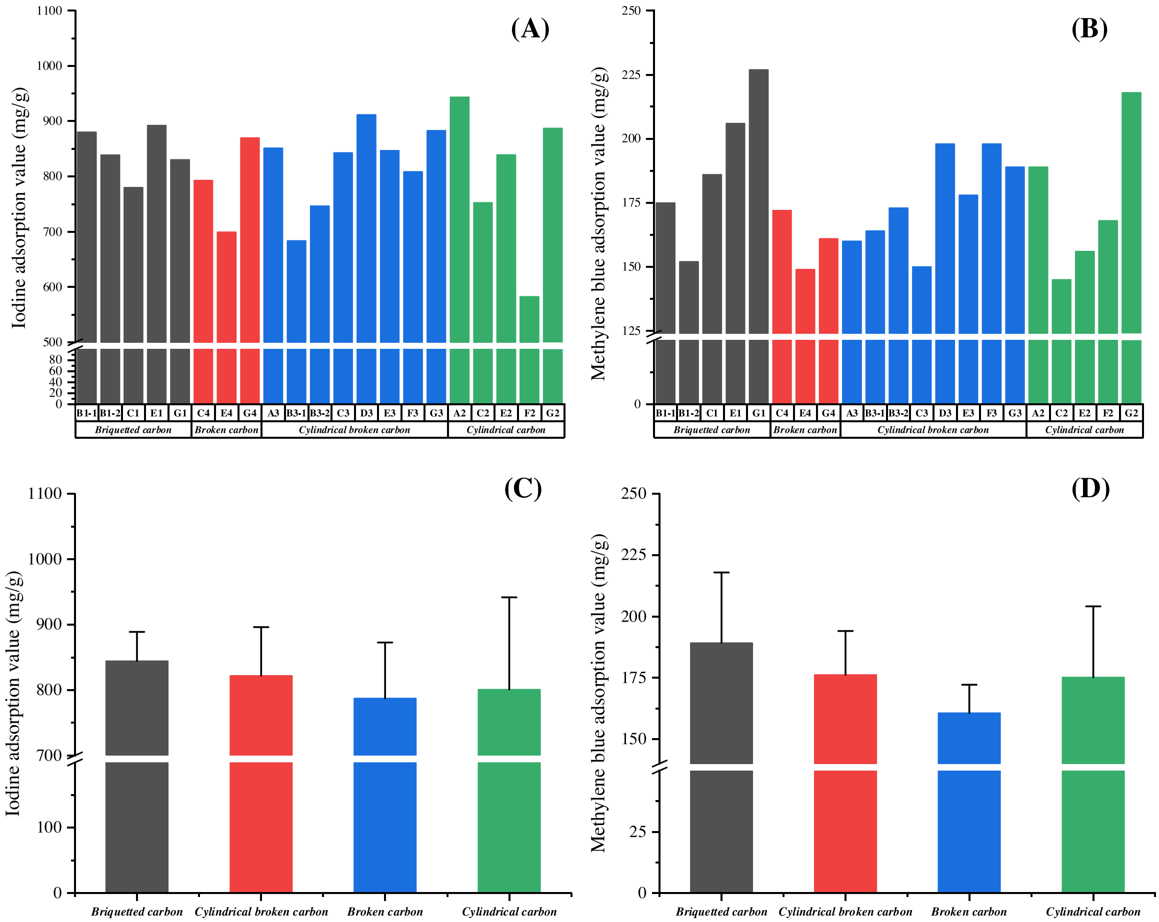

Fig. 2. Static adsorption values of activated carbon.*(A)Iodine adsorption value of 21 kinds of activated carbon. (B)Methylene blue adsorption value of 21 kinds of activated carbon. (C)Iodine adsorption value of four types of activated carbon. (D)Methylene blue adsorption value of four types of activated carbon.*

2.6. Infrared spectroscopy detection of functional groups on the activated carbon surface

A Fourier Transform Infrared Spectrometry Analyzer (Nicolet 5700, Thermo Scientific) was used for the qualitative detection of functional group types on the surface of activated carbon. The scanning range was 400−4000 cm^{-1}, and the resolution was 1 cm^{-1}.

2.7. Boehm titration of functional group content on the activated carbon surface

The most important functional groups on the surface of activated carbon include carboxyl, lactone, carbonyl, and phenolic hydroxyl groups, which are acidic in water and can be quantified by alkaline liquid titration with different intensities. According to the Boehm titration method [26–28], $NaHCO_3$ can neutralize carboxyl groups, Na_2CO_3 can neutralize carboxyl and lactone groups, and NaOH can neutralize carboxyl, lactone, and phenolic hydroxyl groups, so the content of carboxyl, lactone, and phenolic hydroxyl groups can be calculated by titration with $NaHCO_3$, Na_2CO_3, and NaOH solutions, respectively. The operation of the Boehm titration method in this study was modified based on the previous assay.

2.8. The analytic hierarchy process (AHP)

AHP is a systematic and hierarchical analysis method that combines qualitative and quantitative approaches. It is a systematic and hierarchical approach to analyse a system that consists of many factors that are inter-related and inter-constrained and lack of quantitative data. The AHP analysis we used which was divided into four steps: (1) establishing a recursive hierarchy, (2) constructing a judgment matrix in each level, (3) single ranking and consistency check, and (4) total ranking and consistency check. In this study, the decision objective of the hierarchy is the optimal activated carbon selection scheme G. We determined that the criterion layer A contains static adsorption index A_1, dynamic adsorption index A_2, and hardness index A_3. The judgment matrix constructed by comparing the strong and weak relationships between factors on the influence of the decision problem, and the consistency of the test results of the matrix judged by the consistency ratio (CR) and the consistency quantification index (CI).

2.9. Other analytical measurements

A total organic carbon analyzer (TOC-LCPH) was used to measure the DOC of water samples. A UV–vis spectrophotometer (Thermo Evolution 201) was used to measure the UV_{254}. IBM SPSS Statistics-25, conducted with Microsoft Excel software package (Microsoft Corporation, USA), was used to compare the statistical difference between two sets of data. Linear regression was performed using OriginPro 2018 software packages (OriginLab, USA).

3. Results and discussion

3.1. The static adsorption assay

Iodine adsorption values of 21 kinds of activated carbon were shown in Fig. 2A. The iodine adsorption value ranged from 583−944 mg/g, and the average value was 817 mg/g. Methylene blue adsorption values of

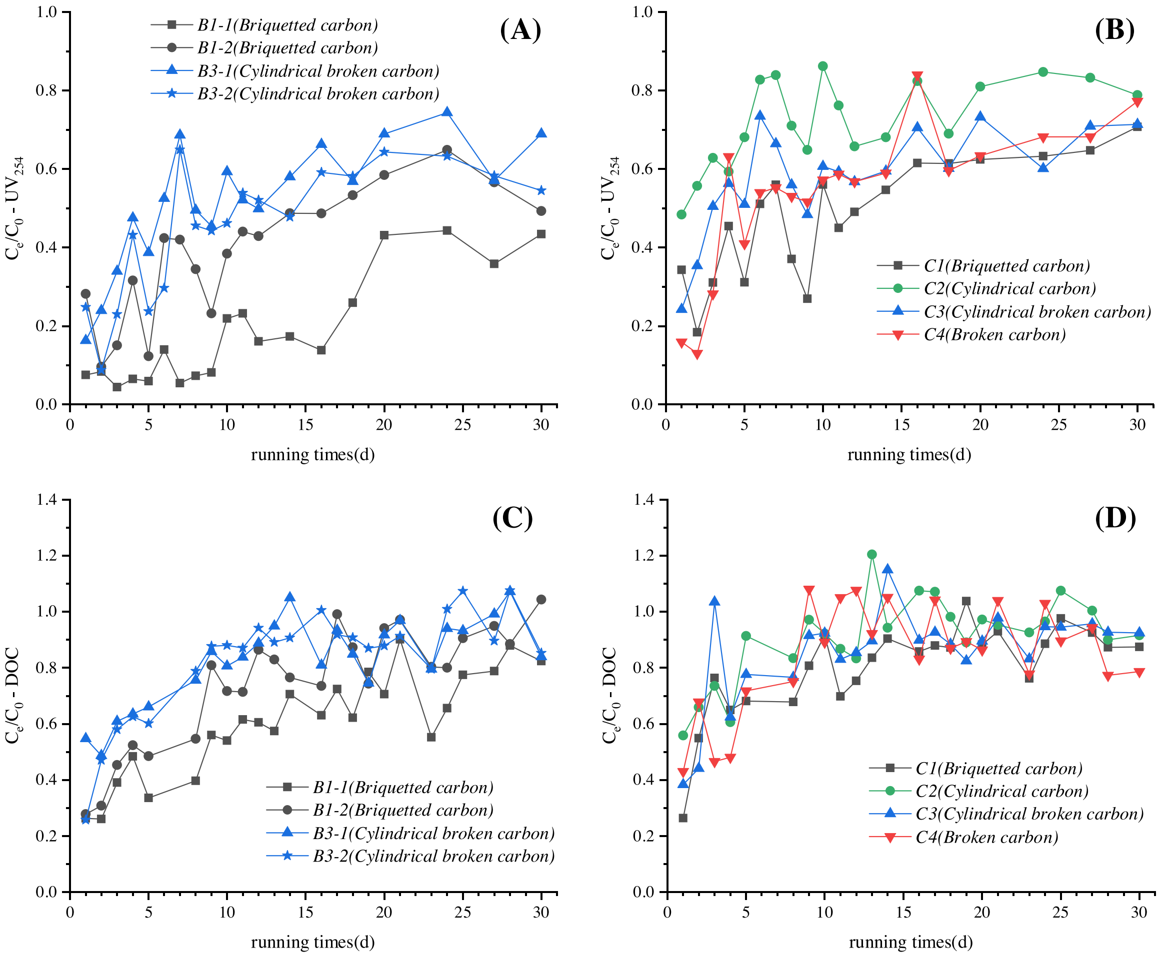

Fig. 3. The C_e/C_0 values of UV_{254} and DOC for different activated carbons.*(A)C_e/C_0- UV_{254}value of activated carbon from company B. (B)C_e/C_0- UV_{254}value of activated carbon from company C. (C)C_e/C_0-DOC value of activated carbon from company B. (D) C_e/C_0-DOC value of activated carbon from company C.*

21 kinds of activated carbon were shown in Fig. 2B. The values of methylene blue adsorption of 21 kinds of activated carbon ranged from 145 to 227 mg/g, and the average value was 177 mg/g.

The iodine value is closely related to the ability of activated carbon to adsorb small molecules. It can be used to estimate the specific surface area of the activated carbon and to relatively characterize the pore structure of the activated carbon. As shown in Fig. 2C, the order was briquetted carbon>cylindrical broken carbon > cylindrical carbon- > broken carbon.

The methylene blue value of liquid-phase adsorption of activated carbon mainly reflects the decoloring ability of the activated carbon, with a higher value indicating better adsorption performance. Methylene blue adsorption values of the four types of activated carbon were equivalent($P > 0.05$). The order was briquetted carbon>cylindrical broken carbon > cylindrical carbon > broken carbon, as shown in Fig. 2D.

The adsorption performance index values of briquetted carbon were higher than those of the other three types of activated carbon, reached or approached the national standard of superior activated carbon. The results showed a large number of micropores, mesopores, and macropodids and a highly developed pore structure. The iodine value of broken carbon was only 788 mg/g, which obviously could not reach the requirement of qualified products, and its value of methylene blue (161 mg/g) was the lowest among the four types of activated carbon, even though it slightly exceeded the qualified line, it indicated that compared with the other three types of activated carbon, the activation degree of broken carbon was lower and the pore structure was less developed.

3.2. The dynamic adsorption assay

The example of four activated carbon types from production companies B and C was shown in Fig. 3. During the 30 days' continuous operation of the dynamic adsorption equipment, Similarly, the UV_{254} and DOC removal efficiencies of the different types of activated carbon columns were high at the beginning of the operation and then gradually decreased, i.e., the values of C_e/C_0 gradually increased (C_e represents the value of effluent UV_{254} and the concentration of effluent DOC, C_0 represents the value of influent UV_{254} and the concentration of influent DOC). In particular, cylindrical carbon and cylindrical broken carbon showed the most significant reduction in removal rates. In contrast, the removal of briquetted carbon was relatively excellent. After 14 days of operation, the values of C_e/C_0 reached a relatively stable stage. It showed that the stabilization values of C_e/C_0 for briquetted carbon (B1-1), (B1-2), and (C1) were all lower than those of the other three types of activated carbon, UV_{254} and DOC values of which are all below 0.5 and 0.9, respectively. Briquetted carbon had a shorter time to reach stabilization values, approximately ten days, which were an obvious advantage. There were slight fluctuations in the UV_{254} and DOC removal rates of all four types of activated carbon, mainly due to fluctuations in the quality of the raw water during the assay period.

The average removal efficiency of UV_{254} for 21 kinds of activated carbon was 16.90–77.35 %. As shown in Fig. 4A, briquetted carbon (B1−1) attained a higher UV_{254} removal efficiency (77.35 %). The dynamic adsorption assay was designed to compare the adsorption effect of different activated carbons on organic matter. Therefore, an experimental bench plant was set up in parallel and operated continuously for

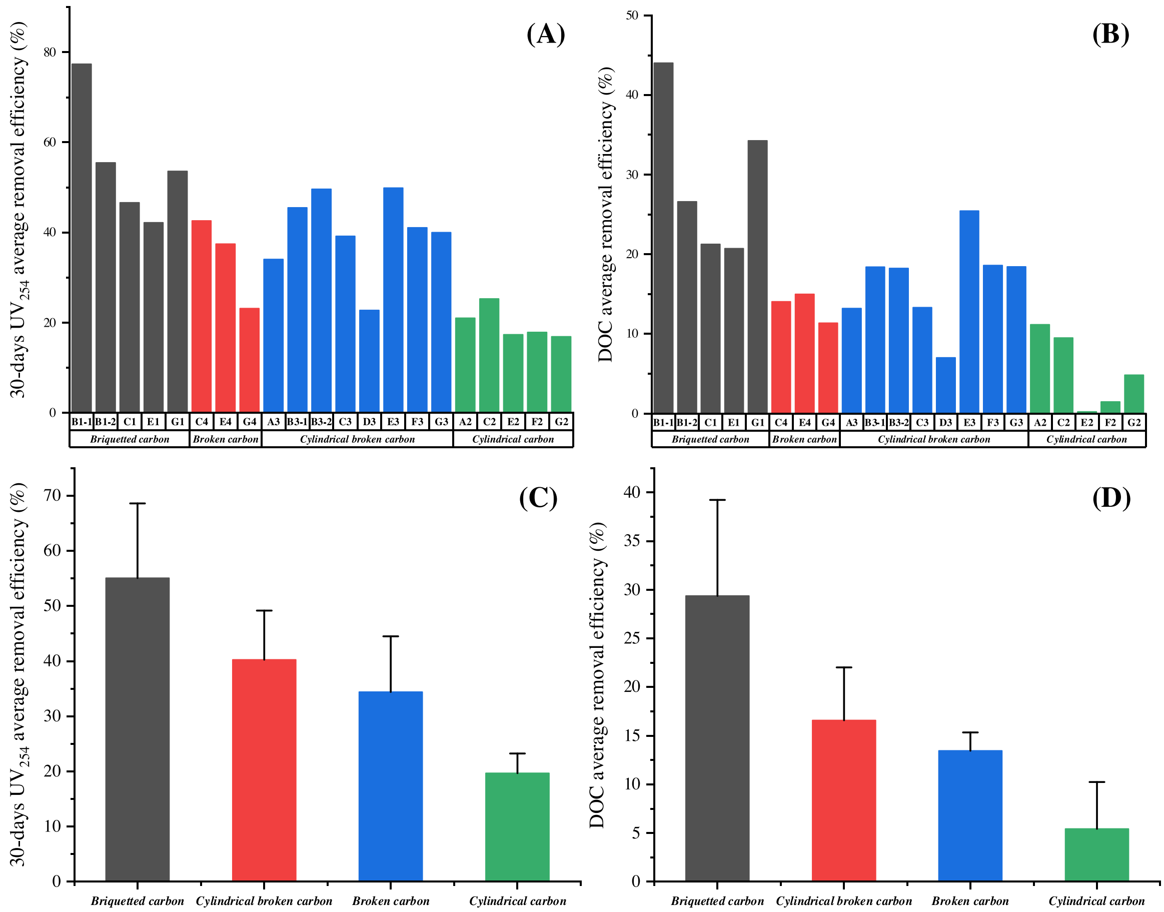

Fig. 4. The dynamic adsorption value of various activated carbon.*(A)30-days average removal efficiency of UV_{254}.(B)30-days average removal efficiency of DOC.(C)the average removal efficiency of UV_{254}. (D)the average removal efficiency of DOC.*

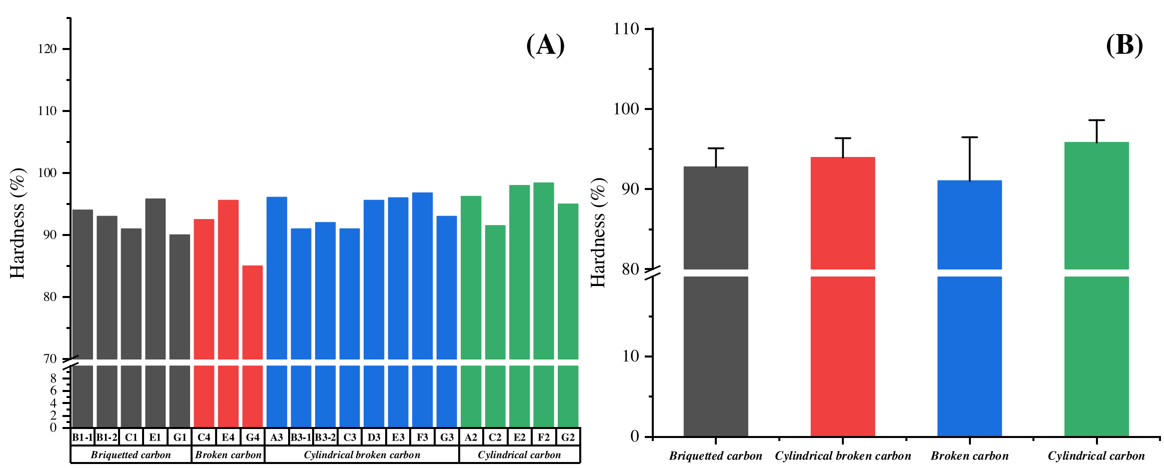

Fig. 5. Hardness values of activated carbon.*(A)the hardness of 21 kinds of activated carbon. (B)the average hardness of four types of activated carbon).*

30 days without backwashing, so the average removal efficiency of DOC was very low. The average removal rate of DOC for different activated carbon ranged from 0.21 to 44.04%, and the briquetted carbon (B1−1) achieved higher DOC removal efficiency (44.04 %). As shown in Fig. 4B, there is a significant difference in the removal effect of DOC on different activated carbons. ($P < 0.05$).

As shown in Fig. 4C and D, the analysis was based on the average removal effect of the four types of activated carbon we selected for DOC and UV_{254}, there is an apparent difference in the average removal efficiency of UV_{254} and DOC between the four types of activated carbon ($P < 0.05$). The order was briquetted carbon>cylindrical broken carbon > broken carbon > cylindrical carbon. The briquetted carbon had a significant advantage, shown by the higher removal efficiency compared with the other three types of carbon ($P < 0.05$). At the same time, the discrepancy between cylindrical broken carbon and broken carbon was minuscule ($P > 0.05$).

3.3. Hardness

The hardness range of 21 kinds of activated carbon was 85–98 %, and the average value was 94 %. As shown in Fig. 5A, the hardness of different activated carbon was equivalent, whose difference was slight ($P > 0.05$).

As the damage of activated carbon during transportation, backwashing and regeneration are considered in the practical application of activated carbon, hardness and coefficient of friction are the primary control indicators in the selection of activated carbon, and it is important to select activated carbon with the hardness and coefficient of friction as high as possible. If the hardness is low, the structure of the carbon is loosened, and it will cause the carbon particles to fall off during backwashing, which will lead to biosecurity issues in the water supply because of the ability of microorganisms to adhere to the surface of the carbon particles. Refer to GB and AWWA standards: hardness values of 90 %. Four types of activated carbon were shown in Fig. 5, briquetted carbon with a hardness range from 90 % to 96 %, and the average value was 93 %, cylindrical broken carbon with a hardness range of 91–97 %, with an average value of 94 %, broken carbon with a hardness range of 85–96 %, with an average value of 91 %, and cylindrical carbon with a hardness range of 92–98 %, with an average value of 96 %. There is little difference in the hardness of the four kinds of activated carbon, and they all met the requirements for application very well ($P > 0.05$).

3.4. Comprehensive evaluation of activated carbon water purification performance

3.4.1. Comprehensive evaluation model for the performance of activated carbon in water purification

Based on the static, dynamic adsorption assay, and the hardness characteristics of 21 kinds of activated carbon. We used the AHP to confirm the weighting coefficient of each factor. A comprehensive evaluation model of the water purification performance of activated carbon had been developed to select the most suitable type of activated carbon.

$$I_i = W_1 \sum_{j=1}^{2} A_{ij} + W_2 \sum_{k=1}^{2} B_{ik} + W_3 C_i \quad (1)$$

I_i —— A comprehensive score of activated carbon, i = 1,2,……21;

W_1—— Static adsorption weighting coefficient,0.33;

W_2 —— Dynamic adsorption weighting coefficient,0.53;

W_3 —— Hardness weighting coefficient,0.14;

A_{ij} —— $A_{ij}(i = 1, 2\ldots, 21; j = 1, 2)$ the normalized score of static adsorption parameters, where the normalized score of iodine adsorption A_{i1}. The normalized score of methylene blue adsorption value A_{i2};

B_{ik} —— $B_{ik}(i = 1, 2\ldots, 21; k = 1, 2)$ the normalized score of dynamic adsorption parameters, in which the value of UV_{254} adsorption is B_{i1}, the value of DOC adsorption is B_{i2};

C_i —— $C_i(i = 1, 2\ldots, 21)$ represents the normalized hardness score.

A_{ij}, B_{ik}, C_i were calculated by the formula:

$$X = \frac{Y - \min\{Z\}}{\max\{Z\}\text{-}\min\{Z\}} \quad (2)$$

X —— A_{ij}, B_{ik}, $C_i(i = 1, 2\ldots, 21; j = 1, 2; k = 1, 2)$;

Y —— a_{ij}, b_{ik}, c_i $(i = 1, 2\ldots, 21; j = 1, 2; k = 1, 2)$;

Z —— a_j, b_k, $c_i(i = 1, 2\ldots, 21; j = 1, 2; k = 1, 2)$;

a_{ij} $(i = 1, 2\ldots, 21; j = 1, 2)$ represents the adsorption value of iodine (j = 1) or methylene blue (j = 2) of activated carbon i;

$b_{ik}(i = 1, 2,\ldots\ldots, 21; k = 1, 2)$ represents the 30-day average removal rate of UV_{254} of activated carbon i (k = 1) or that of DOC (k = 2);

$c_i(i = 1, 2,\ldots\ldots, 21)$ represents the hardness of activated carbon i.

$$\sum_{i=1}^{3} W_i = 1 \quad (3)$$

i = 1,2,3.

The static adsorption performance includes iodine adsorption and methylene blue adsorption. These two parameters may be related to the biomass of microorganisms attached to the activated carbon to some extent [29]. The iodine adsorption and methylene blue adsorption values do not directly characterize the adsorption capacity of activated carbon for natural organics because the iodine and methylene blue values characterize the developed pores with diameters of 1.0 -5.0 nm and 2 -10.1 nm, respectively [30], and the molecules of natural organics are larger than these pores, therefore, the adsorption of natural organics by activated carbon mainly occurs in transition pores with larger pore sizes [29,31]. However, it was found that activated carbon with a larger pore size of 3−10 nm was more effective against removing organic macromolecules, and the biomass attached to activated carbon was closely related to the pore size less than 5 nm ($R > 0.97$) [32], which may be related to the mechanism of biofilm metabolic substrates attached to activated carbon. The substrates were first adsorbed on the pores on the outer surface of activated carbon [33], and it was partially degraded by the biofilm and then diffused into the micropores inside the activated carbon [34], although the bacteria attached to the activated carbon could not enter the micropores. The extracellular enzymes secret by the activated carbon could easily diffuse into the micropores [35]. Under the action of external enzymes and micropores, these substrates partially degraded by the biofilm are further degraded and modified [36], and then desorbed under the movement of the concentration gradient and diffused back to the biofilm to obtain further or complete degradation [37,38]. Therefore, the weight value of activated carbon's static adsorption performance of iodine and methylene blue is relatively large.

With respect to the typical organic metrics, DOC and UV_{254} were chosen as our characterization parameters, where DOC reflects the total amount of soluble organic matter in water [39], and UV_{254} represents the content of humus macromolecular organic matter in water [40] and aromatic compounds containing C=C double bonds and C=O double bonds. In the dynamic adsorption assay, the detection of DOC and UV_{254} in the influent and effluent water of each activated carbon column provides an insight into the removal power of activated carbon for dissolved organic matter and hydrophobicity. Because the dynamic adsorption assay simulates the daily production of a water purification plant, it is more convincing, and its weight value accounts for the largest proportion.

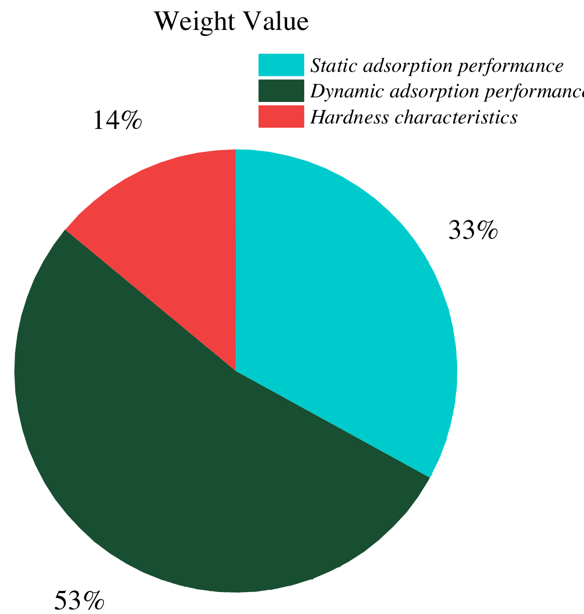

Fig. 6. The weight distribution result of each factor.

Table 2
Comprehensive evaluation calculation table.

Activated carbon type	Ranking	Activated carbon number	Normalized iodide adsorption value	Normalized methylene blue adsorption value	Normalized hardness value	Normalized UV_{254} dynamic adsorption	Normalized DOC dynamic adsorption	comprehensive evaluation
Briquetted carbon	1	B1-1	0.582	0.364	0.672	0.999	1.000	1.561
Briquetted carbon	2	G1	0.440	1.000	0.373	0.606	0.777	1.150
Briquetted carbon	3	B1-2	0.462	0.091	0.597	0.638	0.602	0.983
Cylindrical broken carbon	4	E3	0.484	0.394	0.821	0.545	0.576	0.955
Briquetted carbon	5	E1	0.625	0.742	0.806	0.418	0.468	0.838
Briquetted carbon	6	C1	0.328	0.500	0.448	0.491	0.481	0.808
Cylindrical broken carbon	7	B3-2	0.262	0.333	0.522	0.541	0.412	0.779
Cylindrical broken carbon	8	F3	0.389	0.636	0.881	0.400	0.420	0.764
Cylindrical broken carbon	9	G3	0.592	0.530	0.597	0.382	0.416	0.730
Cylindrical broken carbon	10	B3-1	0.152	0.227	0.448	0.473	0.415	0.705
Broken carbon	11	C4	0.355	0.333	0.560	0.425	0.316	0.643
Cylindrical broken carbon	12	C3	0.473	0.061	0.448	0.369	0.299	0.565
Broken carbon	13	E4	0.178	0.045	0.791	0.340	0.337	0.576
Cylindrical broken carbon	14	A3	0.496	0.182	0.825	0.284	0.296	0.556
Cylindrical carbon	15	A2	1.000	0.530	0.837	0.068	0.250	0.460
Cylindrical broken carbon	16	D3	0.703	0.636	0.791	0.097	0.156	0.390
Broken carbon	17	G4	0.549	0.197	0.000	0.103	0.255	0.325
Cylindrical carbon	18	C2	0.273	0.000	0.485	0.139	0.212	0.322
Cylindrical carbon	19	G2	0.606	0.879	0.746	0.000	0.106	0.297
Cylindrical carbon	20	E2	0.463	0.136	0.970	0.008	0.000	0.163
Cylindrical carbon	21	F2	0.000	0.273	1.000	0.016	0.029	0.159

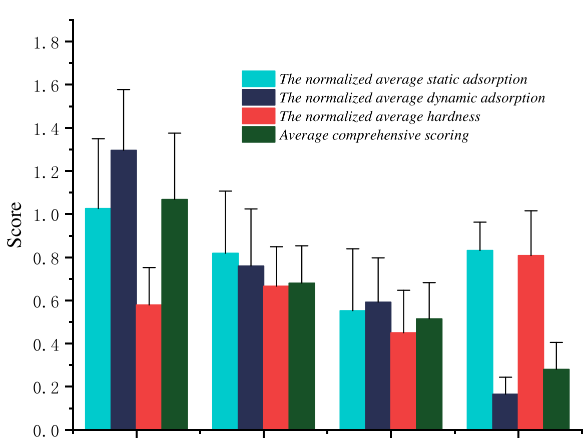

Fig. 7. Comprehensive scoring of four types of activated carbon.

Table 3
Comparison of properties of four types of activated carbon.

Activated carbon category	Advantages	Disadvantages
Briquetted carbon	Best static adsorption capacity and dynamic adsorption capacity; Highest comprehensive performance evaluation	Slightly weaker in hardness
Cylindrical carbon	High hardness and better static adsorption capacity	Weak dynamic adsorption capacity
Cylindrical broken carbon	Good comprehensive performance evaluation	Indicators with no clear advantage
Broken carbon	Good dynamic adsorption capacity	Weak static adsorption capacity; Weak hardness

Table 4
Five kinds of activated carbon pore size and surface area parameters.

Activated carbon type	Average pore size /nm	BET specific area/$m^2 g^{-1}$	The Specific surface area of micropores/ $m^2 g^{-1}$	The Specific surface area of mesoporous/ $m^2 g^{-1}$	The total pore volume /$m^3 g^{-1}$	Micropore volume /$m^3 g^{-1}$	Mesoporous volume /$m^3 g^{-1}$	Comprehensive evaluation
B1-1 (Briquetted carbon)	2.306	1008	804	275	0.581	0.319	0.177	1.561
E3 (Cylindrical broken carbon)	2.021	1036	510	514	0.536	0.212	0.212	0.955
C4 (Broken carbon)	1.966	1063	600	485	0.523	0.242	0.180	0.643
A2 (Cylindrical carbon)	1.941	1104	614	527	0.520	0.240	0.166	0.460
F2 (Cylindrical carbon)	1.805	1007	718	294	0.454	0.288	0.094	0.159

In hardness characteristics analysis, the activated carbon was rubbed, and activated carbon with low strength was prone to cracking during the backwashing process. The pollutants adsorbed by the activated carbon were released into the water, resulting in water quality degradation. Therefore, the hardness of the activated carbon, i.e., the friction resistance of the activated carbon, should also be given sufficient attention. However, since the hardness values of the 21 types of activated carbon in this study were not much different, the weight value of the specific gravity is smaller than that of static adsorption and dynamic adsorption.

We have ranked the weights of the three index factors, dynamic adsorption performance > static adsorption performance > hardness characteristics, and through the analytic hierarchy process [41–44], the following table was obtained:

	Static adsorption performance	Dynamic adsorption performance	Hardness characteristics
Static adsorption performance	1	1/2	3
Dynamic adsorption performance	2	1	3
Hardness characteristics	1/3	1/3	1

The eigenvectors, maximum eigenvalues, CI values, etc., were analyzed and calculated. The final weight distribution result was obtained as Fig. 6 shown.

3.4.2. Comprehensive evaluation results

According to the granular activated carbon optimization model, the total score of 21 kinds of activated carbon was calculated, as showed in Table 2.

The total score range of 21 kinds of activated carbon was 0.159–1.561, and the average value was 0.654. Briquette carbon (B1-1) had the highest normalized score in this category because of its good dynamic adsorption performance, which played an integral part in the model with a weighting of 53 %. In contrast, the performance of cylindrical carbon (F2) was particularly unsatisfactory, as it ranked last in both static and dynamic adsorption performance, even though it had the best hardness properties.

The average comprehensive score of the four types of activated carbon was shown in Fig. 7. The order was briquetted carbon > cylindrical broken carbon > broken carbon > cylindrical carbon. A visual comparison of the performance advantages and disadvantages of the four types of activated carbon we selected is shown in Table 3.

3.5. Validation of the comprehensive evaluation model for activated carbon water purification performance

Based on the results of the comprehensive Evaluation Ranking, the sample of activated carbon with the highest overall rating in each category (B1-1, E3, C4, A2) which belong to briquetted carbon, cylindrical broken carbon, broken carbon, and cylindrical carbon, respective, and the one at the bottom of the ranking of 21 activated carbons (F2), which were selected for physical and chemical property analysis.

3.5.1. Pore size and surface area parameters

The BET surface area and pore size distribution of five kinds of activated carbon numbered B1-1, E3, C4, A2, and F2 were tested, and the results were shown in Table 4.

The average pore diameter of five kinds of activated carbon was between 1.8–2.3 nm. As it ranked first in the total score, the average pore diameter of B1-1 (briquetted carbon) was higher than other activated carbon. Data statistics showed that the average pore size of activated carbon was related to the total score ($P<0.01$). The larger the average pore size, the higher the comprehensive score ranking.

The BET surface area of the five activated carbon types was comparable, with the largest surface area being A2 (cylindrical carbon) at 1104 m^2/g and the smallest being F2 (cylindrical carbon) at 1007 m^2/g. The ranking order of the surface area was A2 (cylindrical carbon)>C4 (broken carbon)>E3 (cylindrical broken carbon)>B1-1 (briquetted carbon)>F2 (cylindrical carbon).

The differences in total pore volume were noticeable. The largest total pore volume was 0.581 m^3/g for briquetted carbon B1-1 (briquetted carbon), and the smallest was 0.454 m^3/g for F2 (cylindrical carbon). The order of total pore volume was B1-1 (briquetted carbon)> E3 (cylindrical broken carbon)>C4 (broken carbon)>A2 (cylindrical carbon)>F2 (cylindrical carbon).

The five kinds of activated carbon mentioned above had well-developed micropores, but there is a wide variation among the activated carbon types, B1-1 (briquetted carbon) had the largest micropore surface area of 804 m^2/g, and E3 (cylindrical broken carbon) had the smallest micropore volume of 510 m^2/g, B1-1 (briquetted carbon) had the largest micropore volume of 0.319 m^3/g and E3 (column broken carbon) had the smallest micropore volume of 0.212 m^3/g. The largest mesopore-specific surface area was A2 (cylindrical carbon) with 527 m^2/g, and the smallest was B1-1 (briquetted carbon) with 275 m^2/g. The largest mesopore volume was E3 (cylindrical broken carbon) with 0.212 m^3/g, and the smallest was F2 (cylindrical carbon) with 0.094 m^3/g.

3.5.2. The surface functional group of activated carbon

The Fourier transform infrared spectrometry was used to analyze the surface functional groups of activated carbon qualitatively. As shown in Fig. 8, it demonstrated that the infrared spectra of A2, B1-1, C4, and E3 were similar, with absorption peaks near 1600 cm^{-1} and 3250−3600 cm^{-1}. The absorption peak at 1600 cm^{-1} might be caused by C═O of non-conjugated ketones, carboxyl groups, or lactone groups. The absorption peak near 3250−3600 cm^{-1} was dense and obvious. The absorption peak near 3250 cm^{-1} might be caused by crystallization water, the absorption peak at 3400 cm^{-1} mainly resulted from the

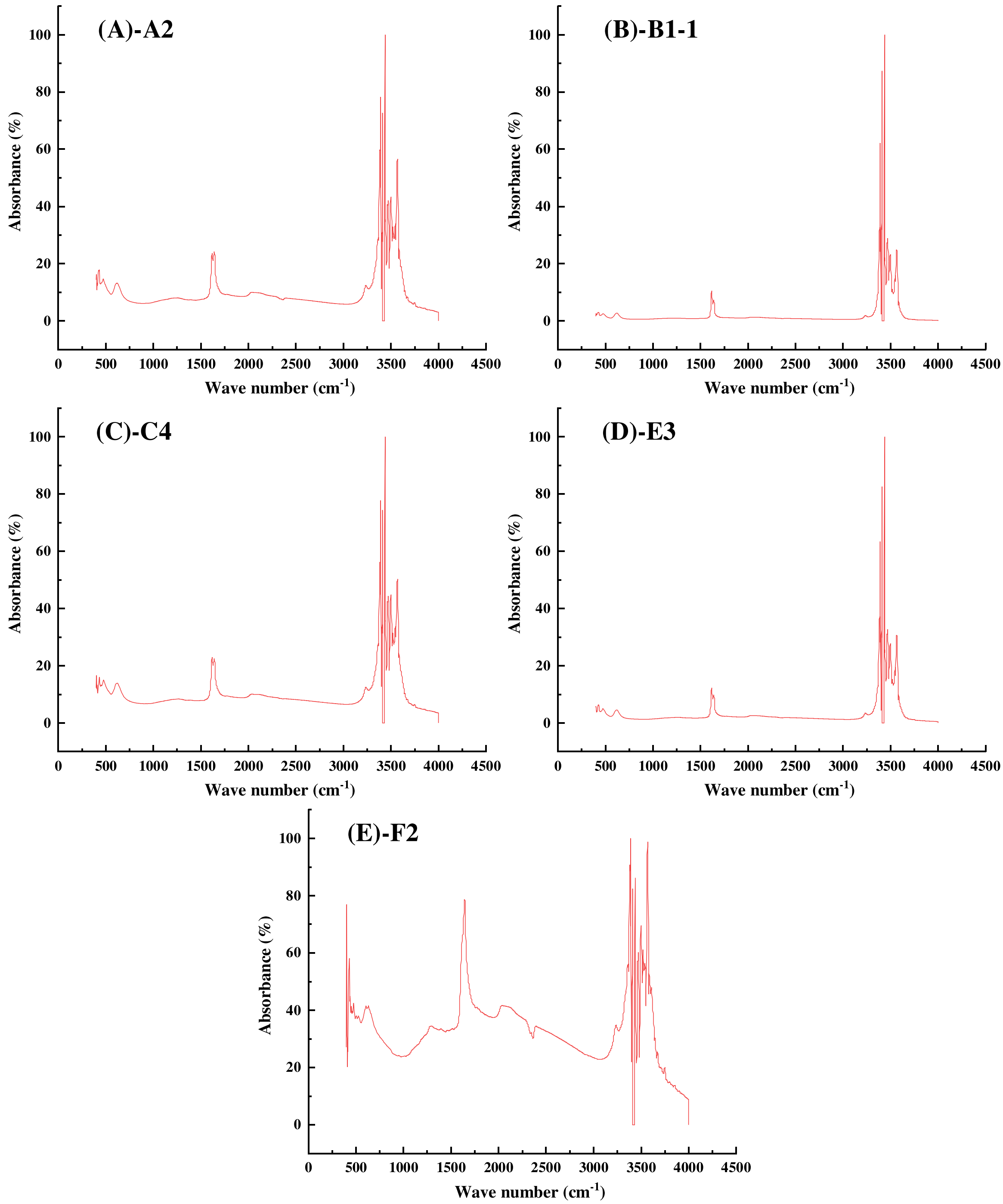

Fig. 8. Fourier infrared spectrum of five kinds of activated carbon.

Table 5
Five kinds of activated carbon surface functional group content.

Type of activated carbon	Carboxy group /mmol g^{-1}	Lactones group /mmol g^{-1}	Phenolic hydroxyl group /mmol g^{-1}	Acidic groups /mmol g^{-1}	comprehensive evaluation
B1-1 (briquetted carbon)	2.895	0.192	0.902	3.988	1.561
E3 (cylindrical broken carbon)	2.949	0.507	0.325	3.781	0.955
C4 (broken carbon)	2.977	0.632	0.143	3.753	0.643
A2 (cylindrical carbon)	1.946	0.183	0.639	2.768	0.460
F2 (cylindrical carbon)	1.632	0.406	0.234	2.271	0.159

stretching vibration of —OH, which might be a carboxyl group and phenolic hydroxyl group, the absorption peak at 3640 cm^{-1} was primarily driven by structured water. In addition to the absorption peak, the F2 spectrum also had an absorption peak near 2000 cm^{-1} which arose from C≡C.

According to the Boehn titration method [26–28], the content of surface functional groups in five activated carbon materials was shown in Table 5. It indicated that the content of acidic oxygen-containing functional groups in descending order was B1-1 (briquetted carbon)> E3 (cylindrical broken carbon)>C4 (broken carbon)>A2 (cylindrical carbon)>F2 (cylindrical carbon). The content of acidic oxygen-containing functional groups of activated carbon correlated with the total score. The contents of the carboxyl group, lactone group, and phenolic hydroxyl group between different activated carbons were quite different. The carboxyl group content was sorted as C4 (broken charcoal)>E3 (cylindrical broken carbon)>B1-1 (briquetted carbon)> A2 (cylindrical carbon)>F2 (cylindrical carbon), and the lactone group content was in the order of C4 (broken carbon)>E3 (cylindrical broken carbon)>F2 (cylindrical carbon)>B1-1 (briquetted carbon)>A2 (cylindrical carbon), the phenolic hydroxyl group content in descending order was B1-1 (briquetted carbon)>A2 (cylindrical carbon)>E3 (cylindrical broken carbon)>F2 (cylindrical carbon)>C4 (broken carbon).

In summary, according to the analysis of the physical and chemical properties of activated carbon, there is no obvious difference in the specific surface area and the types of surface functional groups among the five types of activated carbon. The overall score of activated carbon based on the evaluation model developed in this study was correlated with the average pore size of activated carbon ($P < 0.05$). In other words, the higher the composite score was, the larger the average pore size was. Besides, the overall score correlates with the size of the total pore volume and the amount of acidic oxygenated functional groups on the surface. The total pore volume and acidic oxygenated functional group content show an increasing trend as the overall score increases.

4. Conclusion

The objective of this research was to develop a comprehensive evaluation model for the water purification performance of activated carbon, which based on its static adsorption (iodine adsorption and methylene blue adsorption), dynamic adsorption (DOC and UV_{254} removal efficiency), and hardness (abrasion resistance), and to define a selection method to select the optimal carbon from among the various activated carbon types. It had been proved that the overall score of briquetted carbon was higher than the other three types of activated carbon. The developed evaluation model was validated by the physical and chemical properties of the activated carbon. It had been demonstrated that the comprehensive evaluation model developed in this study has a remarkable relationship to the average pore size of the activated carbon ($P < 0.05$). The validity of the comprehensive evaluation model was demonstrated by the specific correlation of the total score of the total pore size and the surface acidic oxygen functional group content of the activated carbon. It means that the higher the composite score was, the larger the average pore size was and the larger the total pore size and the surface acidic oxygen functional group content of the activated carbon was. This method of optimized selection could provide theoretical and practical support for the carbon selection step in the O_3-BAC treatment process.

Declaration of Competing Interest

There is no conflict of interest.

Acknowledgments

We are grateful for the cooperation and participation of the utilities involved in this project, supported by the National Nature Science Foundation of China (Project NO. 51979194). We also thank the research on water quality stability characteristics and countermeasures of the Fuzhou Water Supply System (Project NO. 20203000) from Fuzhou Water Group Co. Ltd, China.

Appendix A. Supplementary data

Supplementary material related to this article can be found, in the online version, at doi:https://doi.org/10.1016/j.jwpe.2021.101931.

References

[1] Z.A. Alothman, M.R. Khan, S.M. Wabaidur, M.R. Siddiqui, Persistent organic pollutants: overview of their extraction and estimation, Sens. Lett. 10 (2012) 698–704.
[2] M. Naushad, M.R. Khan, Z.A. Alothman, M.R. Awual, Bromate removal from water samples using strongly basic anion exchange resin Amberlite IRA-400: kinetics, isotherms and thermodynamic studies, Desalin. Water Treat. 57 (2016).
[3] I.H. Alsohaimi, M.A. Khan, Z.A. Alothman, M.R. Khan, M. Kumar, A.M.A. Mahri, Synthesis, characterization, and application of Fe-CNTs nanocomposite for BrO_3-remediation from water samples, J. Ind. Eng. Chem. 26 (2015).
[4] M. Naushad, Z.A. Alothman, M.R. Khan, N.J. Alqahtani, I.H. Alsohaimi, Equilibrium, kinetics and thermodynamic studies for the removal of organophosphorus pesticide using Amberlyst-15 resin: quantitative analysis by liquid chromatography-mass spectrometry, J. Ind. Eng. Chem. 20 (2014).
[5] M. Naushad, M.A. Khan, Z.A. Alothman, M.R. Khan, Adsorptive removal of nitrate from synthetic and commercially available bottled water samples using De-Acidite FF-IP resin, J. Ind. Eng. Chem. 20 (2014).
[6] M. Naushad, Z.A. Alothman, M.R. Khan, Removal of malathion from aqueous solution using De-Acidite FF-IP resin and determination by UPLC-MS/MS: equilibrium, kinetics and thermodynamics studies, Talanta 115 (2013).
[7] A.A. Alqadami, M. Naushad, M.A. Abdalla, M.R. Khan, Z.A. Alothman, Adsorptive removal of toxic dye using Fe_3O_4-TSC nanocomposite: equilibrium, Kinetic, and thermodynamic studies, J. Chem. Eng. Data 61 (2016) 3806–3813.
[8] S. Hussain, J. Awad, B. Sarkar, C.W.K. Chow, J. Duan, J. van Leeuwen, Coagulation of dissolved organic matter in surface water by novel titanium (III) chloride: Mechanistic surface chemical and spectroscopic characterisation, Sep. Purif. Technol. 213 (2019).
[9] C. Li, D. Wang, X. Xu, M. Xu, Z. Wang, R. Xiao, Tracking changes in composition and amount of dissolved organic matter throughout drinking water treatment plants by comprehensive two-dimensional gas chromatography-quadrupole mass spectrometry, Sci. Total Environ. 609 (2017).
[10] P. Lin, Y. Zhang, X. Zhang, C. Chen, Y. Xie, I.H. Suffet, The influence of chlorinated aromatics' structure on their adsorption characteristics on activated carbon to tackle chemical spills in drinking water source, Front. Environ. Sci. Eng. 9 (2015).
[11] M. Naushad, M.R. Khan, Z.A. Alothman, A.H.A. Muhtaseb, M.R. Awual, A. A. Alqadami, Water purification using cost effective material prepared from agricultural waste: kinetics, isotherms, and thermodynamic studies, Clean-Soil, Air, Water 44 (2016).
[12] M. Naushad, M.R. Khan, Z.A. Alothman, I. AlSohaimi, F. Rodriguez-Reinoso, T. M. Turki, R. Ali, Removal of BrO^{3-} from drinking water samples using newly developed agricultural waste-based activated carbon and its determination by ultra-performance liquid chromatography-mass spectrometry, Environ. Sci. Pollut. Res. Int. 22 (2015) 15853.
[13] P.R.D. Santos, L.A. Daniel, A review: organic matter and ammonia removal by biological activated carbon filtration for water and wastewater treatment, Int. J. Environ. Sci. Technol. 17 (2020).
[14] D.M. Golea, P. Jarvis, B. Jefferson, G. Moore, S. Sutherland, S.A. Parsons, S.J. Judd, Influence of granular activated carbon media properties on natural organic matter and disinfection by-product precursor removal from drinking water, Water Res. 174 (2020).
[15] S. Hong, F. Hongliang, W. Nanxiang, H. Jun, A comparison of removal efficiencies of conventional drinking water treatment and advanced treatment equipped with ozone-biological activated carbon process, Environ. Technol. (2020).
[16] I.V. Kumpanenko, N.A. Ivanova, M.V. Dyubanov, O.V. Shapovalova, A.A.S. Yanov, A.V. Roshchin, Analysis of breakthrough curves of dynamic adsorptive removal of pollutants from water, Russ. J. phys. Chem. B 13 (2019).
[17] S. Jaman, R. Rodriguez, D.W. Mazyck, Evaluation of common granular activated carbon parameters for trace contaminant removal, J. Environ. Eng. 145 (2019).
[18] M. Naushad, M.A. Khan, Z.A. Alothman, M.R. Khan, M. Kumar, Adsorption of methylene blue on chemically modified pine nut shells in single and binary systems: isotherms, kinetics, and thermodynamic studies, Desalin. Water Treat. 57 (2016).
[19] M.A. Khan, Z.A. Alothman, M. Naushad, M.R. Khan, M. Luqman, Adsorption of methylene blue on strongly basic anion exchange resin (Zerolit DMF): kinetic, isotherm, and thermodynamic studies, Desalin. Water Treat. 53 (2015).
[20] F. Zietzschmann, J. Altmann, A.S. Ruhl, U. Dünnbier, I. Dommisch, A. Sperlich, F. Meinel, M. Jekel, Estimating organic micro-pollutant removal potential of activated carbons using UV absorption and carbon characteristics, Water Res. 56 (2014).
[21] D.J. de Ridder, A.R.D. Verliefde, K. Schoutteten, B. van der Linden, S.G.J. Heijman, I. Beurroies, R. Denoyel, G.L. Amy, J.C. van Dijk, Relation between interfacial

energy and adsorption of organic micropollutants onto activated carbon, Carbon (2012).
[22] I.A.Q.O. General Administration of Quality Supervision, C.N.S.M. Committee, in: I. A.Q.O. General Administration of Quality Supervision (Ed.), Test Method for Granular Activated Carbon From Coal-DetermiNation of Iodine Adsorption [M], Standards Press of China, BeiJing, 2008.
[23] M.R. Khan, M.A. Khan, Z.A. Alothman, I.H. Alsohaimi, M. Naushad, N.H. Al-Shaalan, Quantitative determination of methylene blue in environmental samples by solid-phase extraction and ultra-performance liquid chromatography-tandem mass spectrometry: a green approach, RSC Adv. 4 (2014) 34037–34044.
[24] I.A.Q.O. General Administration of Quality Supervision, C.N.S.M. Committee, in: I. A.Q.O. General Administration of Quality Supervision (Ed.), Test Method for Granular Activated Carbon From Coal-Determination of Methylene Blue Adsorption [M], Standards Press of China, Beijing, 2008.
[25] I.A.Q.O. General Administration of Quality Supervision, C.N.S.M. Committee, in: I. A.Q.O. General Administration of Quality Supervision (Ed.), Test Method for Granular Activated Carbon From Coal-Determination of Hardness [M]., Standards Press of China, BeiJing, 2008.
[26] S. Ma, H. Li, G. Zhang, T. Iqbal, K. Li, Q. Lu, Catalytic fast pyrolysis of walnut shell for alkylphenols production with nitrogen-doped activated carbon catalyst, Front. Environ. Sci. Eng. 15 (2020).
[27] M. hernandez-ortiz, H.A. durán-muñoz, J.D. lozano-lópez, S.M. durón, M. galván-valencia, Y. estevez-martínez, I. ortiz-medina, L.A. ramírez-hernández, O. cruz-domínguez, V.M. castaño, Determination of the surface functionality of nanocarbon allotropes by boehm titration, Surf. Rev. Lett. 27 (2020).
[28] Y.S. Kim, S.J. Yang, H.J. Lim, T. Kim, C.R. Park, A simple method for determining the neutralization point in Boehm titration regardless of the CO_2 effect, Carbon 50 (2012).
[29] S. Yin, Y. Chen, Y. Li, W. Cen, H. Yin, Static and dynamic characteristics of SO_2-O_2 aqueous solution in the microstructure of porous carbon materials, Front. Environ. Sci. Eng. 12 (2018).
[30] W. Qi, W. Li, J. Zhang, X. Wu, J. Zhang, W. Zhang, Effect of biological activated carbon filter depth and backwashing process on transformation of biofilm community, Front. Environ. Sci. Eng. 13 (2019).
[31] Y. Shimizu, M. Ateia, C. Yoshimura, Natural organic matter undergoes different molecular sieving by adsorption on activated carbon and carbon nanotubes, Chemosphere 203 (2018).
[32] J.H. Noh, S.H. Yoo, H. Son, K.E. Fish, I. Douterelo, S.K. Maeng, Effects of phosphate and hydrogen peroxide on the performance of a biological activated carbon filter for enhanced biofiltration, J. Hazard. Mater. 388 (2020).
[33] L. Pan, Y. Takagi, Y. Matsui, T. Matsushita, N. Shirasaki, Micro-milling of spent granular activated carbon for its possible reuse as an adsorbent: remaining capacity and characteristics, Water Res. 114 (2017).
[34] P. Laura, J.E. Dykstra, M.G. Adishaktia, B. Marco, A.A.M. Langenhoff, Albert van der Wal, Diffusion of hydrophilic organic micropollutants in granular activated carbon with different pore sizes, Water Res. 162 (2019).
[35] S.M. Korotta-Gamage, A. Sathasivan, A review: potential and challenges of biologically activated carbon to remove natural organic matter in drinking water purification process, Chemosphere 167 (2017).
[36] N. Klimenko, M. Winther-Nielsen, S. Smolin, L. Nevynna, J. Sydorenko, Role of the physico-chemical factors in the purification process of water from surface-active matter by biosorption, Water Res. 36 (2002).
[37] Y. Salama, M. Chennaoui, A. Sylla, M. Mountadar, M. Rihani, O. Assobhei, Characterization, structure, and function of extracellular polymeric substances (EPS) of microbial biofilm in biological wastewater treatment systems: a review, Desalin. Water Treat. 57 (2016).
[38] S. Smolin, I. Kozyatnyk, N. Klymenko, New approach for the assessment of the contribution of adsorption, biodegradation and self-bioregeneration in the dynamic process of biologically active carbon functioning, Chemosphere 248 (2020).
[39] W. Xing, H.H. Ngo, S.H. Kim, W.S. Guo, P. Hagare, Adsorption and bioadsorption of granular activated carbon (GAC) for dissolved organic carbon (DOC) removal in wastewater, Bioresour. Technol. Rep. 99 (2008).
[40] Y. Li, Ozone biological activated carbon advanced removal typical persistent organic pollutants from micropolluted source water yangtze delta region, Probe-Environ. Sci. Technol. 1 (2019).
[41] Y.J. Mo, L.S. Gu, A mathematical theory of the AHP(Analytic Hierarchy Process) and its application to assess research proposals, Commun. Math. Educ. 22 (2008).
[42] Y. Liu, C.M. Eckert, C. Earl, A review of fuzzy AHP methods for decision-making with subjective judgements, Expert Syst. Appl. 161 (2020).
[43] E. Mastrocinque, F.J. Ramírez, A. Honrubia-Escribano, Duc T. Pham, An AHP-based multi-criteria model for sustainable supply chain development in the renewable energy sector, Expert Syst. Appl. 150 (2020).
[44] Y.J. Mo, L.S. Gu, A mathematical theory of the AHP(Analytic Hierarchy Process) and its application to assess research proposals, Commun. Math. Educ. 22 (2008).